

PROTEIN ANALYSIS BY HYDROGEN EXCHANGE MASS SPECTROMETRY

Andrew N. Hoofnagle,¹ Katheryn A. Resing,¹
and Natalie G. Ahn^{1,2}

¹*Department of Chemistry and Biochemistry and* ²*Howard Hughes Medical Institute, University of Colorado, Boulder, Colorado 80309; email: Andrew.Hoofnagle@uchsc.edu; Katheryn.Resing@colorado.edu; Natalie.Ahn@colorado.edu*

Key Words protein dynamics, folding, allostery, electrospray ionization, matrix-assisted laser desorption ionization

■ **Abstract** Mass spectrometry has provided a powerful method for monitoring hydrogen exchange of protein backbone amides with deuterium from solvent. In comparison to popular NMR approaches, mass spectrometry has the advantages of higher sensitivity, wider coverage of sequence, and the ability to analyze larger proteins. Proteolytic fragmentation of proteins following the exchange reaction provides moderate structural resolution, in some cases enabling measurements from single amides. The technique has provided new insight into protein-protein and protein-ligand interfaces, as well as conformational changes during protein folding or denaturation. In addition, recent studies illustrate the utility of hydrogen exchange mass spectrometry toward detecting protein motions relevant to allostery, covalent modifications, and enzyme function.

CONTENTS

INTRODUCTION	2
THEORY	2
HISTORICAL PERSPECTIVE	6
TECHNIQUES	8
Data Collection	9
Data Reduction	11
STRUCTURAL RESOLUTION	13
Increased Resolution Achieved with Overlapping Peptides	13
Tandem Mass Spectrometry	14
APPLICATIONS	16
Folding and Stability	16
Ligand Binding, Aggregation, and Protein-Protein Interactions	17
Dynamics	18
CONCLUSIONS	20

INTRODUCTION

Hydrogen exchange at protein backbone amides was first analyzed by scintillation counting, infrared and ultraviolet spectroscopies, neutron diffraction, and nuclear magnetic resonance (NMR) spectroscopy. Recent advances in mass spectrometry (MS) allow increased sensitivity and the ability to analyze larger proteins and protein complexes than currently possible with NMR, although generally at the cost of reduced structural resolution. This review surveys the theory of hydrogen exchange, the methods for hydrogen exchange mass spectrometry (HX-MS), and the application to various biophysical problems, including folding and conformational changes. Special attention is paid to new insights into protein dynamics provided by HX-MS.

THEORY

In short peptides, amide hydrogen exchange involves proton abstraction described by a chemical exchange rate (k_{ch}) for a second-order reaction that depends on an “intrinsic” rate of exchange for that hydrogen (k_{int}) as well as the concentration of available catalyst, including OH^- , H_3O^+ , water, and acidic or basic solutes ($k_{\text{ch}} = k_{\text{int}} [\text{catalyst}]$) (Figure 1*a*). The chemical exchange rate is minimal near $\text{pH}_{\text{read}} 2.5$. Below this pH, exchange occurs via proton addition, catalyzed by D_3O^+ . Above this pH, exchange occurs by proton abstraction predominantly catalyzed by OH^- . Because chemical exchange rates of amide deuterium and tritium are slower than hydrogen, with little solvent isotope effect, proton abstraction is rate limiting in reactions above $\text{pH}_{\text{read}} 2.5$ (9, 16). Importantly, the chemical exchange rate is also influenced by the amino acid sequence surrounding an amide hydrogen in two ways. First, the intrinsic rate of exchange for that hydrogen (k_{int}) depends on local inductive effects of adjacent side chains that alter the pKa of the hydrogen atom. Second, the local concentration of available catalyst can be altered by the presence of adjacent reactive side chain groups. The inductive, catalytic, and steric effects of adjacent residues on amide chemical hydrogen exchange rates in peptides have been elegantly quantified by Bai et al. (8), whose analysis allows rapid calculation of chemical exchange rates of peptide amide hydrogen atoms based on sequence.

Although chemical exchange occurs rapidly for amide hydrogens in peptides at neutral pH ($k_{\text{ch}} \sim 10^1 - 10^3 \text{ sec}^{-1}$), observed exchange of backbone amide hydrogens in proteins can occur much more slowly, with half lives ranging from milliseconds to years. The exchange rate of a given proton depends on two factors. The most important factor is the degree of solvent protection and hydrogen bonding within the protein. In general, hydrogen exchange rates are slower when protons are removed from the solvent-protein interface and when more stable hydrogen bond contacts are made with surrounding residues in the secondary and tertiary structure (62).

Because higher-order structure has such a profound role, hydrogen exchange is markedly affected by protein flexibility and mobility (9, 27, 38). Even protons that

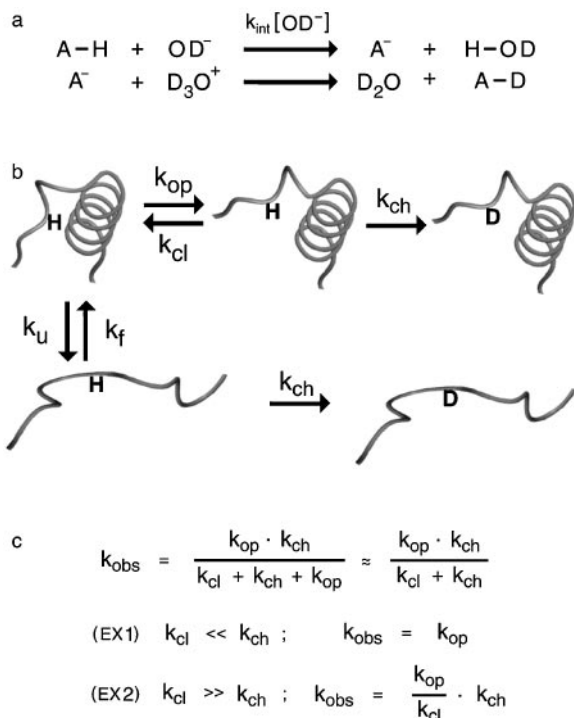


Figure 1 Mechanism of hydrogen exchange. (a) Amide exchange at neutral pH involves base catalyzed proton abstraction and acid catalyzed transfer of deuterium from solvent. Measurable isotope effects on the amide hydrogen and a lack of a solvent isotope effect indicate that proton abstraction is rate limiting. (b) Hydrogen exchange of a buried amide is facilitated by different mechanisms, involving small-amplitude fluctuations (*upper pathway*) on one extreme, and complete unfolding (*lower pathway*) on the other. The observed rate of exchange (k_{obs}) for small-amplitude fluctuations is a function of the rate of structural opening (k_{op}), the rate of structural closing (k_{cl}), and the chemical rate of exchange ($k_{\text{ch}} = k_{\text{int}}$ [catalyst]), where catalyst is OH^- or buffer. In native proteins, the rate of opening is assumed to be much slower than the rate of closing, which results in a simplified rate expression (upper equation, *far right*). The observed rates of small-amplitude fluctuations lie on a continuum described by EX1 and EX2 conditions, as described in the text.

are highly buried or hydrogen bonded can exchange through fluctuations in the molecule that allow transient solvent penetration. The amplitude of these fluctuations can be small enough to involve the breaking of a single hydrogen bond or large enough to involve complete unfolding of the protein (4, 15, 69). Many hydrogens exchange by mechanisms involving small-amplitude fluctuations and may include low-energy explorations of conformational space as well as higher-energy local

unfolding events. These can be described by equilibria between solvent-exposed versus solvent-protected states, governed by rate constants for opening and closing (k_{op} , k_{cl}) (Figure 1*b*, upper pathway). On the other hand, hydrogens buried in the middle of large stable protein domains exchange by mechanisms involving complete unfolding (Figure 1*b*, lower pathway), which are enhanced in the presence of heat or denaturants (7, 26).

The small-amplitude fluctuations that convert solvent-protected hydrogens to solvent-exposed (Figure 1*b*, upper pathway) are assumed to be completely reversible (6, 15, 27, 38). They represent a continuum of hydrogen exchange mechanisms: At one end of the continuum (termed the EX1 regime), chemical exchange occurs quickly after conversion to the solvent-exposed form, and the observed rate (k_{obs}) can be described by the rate of structural opening ($k_{\text{obs}} = k_{\text{op}}$) (15, 27) (Figure 1*c*). These motions can be described as local unfolding events and occur on timescales of milliseconds to days. In general, local unfolding involves many residues of the protein and leads to simultaneous solvent exposure of many amides (4, 28, 69). At the other end (termed EX2), reconversion of the solvent-exposed form back to the protected form occurs much faster than the rate of chemical exchange. These motions can be described as native state fluctuations or protein breathing motions, assumed to occur on timescales of microseconds to milliseconds. In this extreme, k_{obs} depends on the equilibrium of protected and exposed forms and on the chemical exchange rate ($k_{\text{obs}} = k_{\text{op}}/k_{\text{cl}} \cdot k_{\text{ch}}$) (15, 27) (Figure 1*c*). Thus, hydrogen exchange measurements reveal information about folding as well as internal motions of the folded state.

Because the chemical exchange rate is proportional to hydroxide ion concentration (Figure 1*a*), the pH dependence of observed hydrogen exchange rates reveals where protein motions reside on the continuum between EX1 and EX2. In the EX1 regime, k_{obs} is independent of chemical exchange, and in most cases complete pH independence will be observed provided that protein structure and the opening and closing rates are not affected by pH (Figure 1*b,c*). On the other hand, k_{obs} is strongly pH dependent in the EX2 regime because the observed rate is directly proportional to the chemical exchange rate (Figure 1*b,c*). For native state proteins, experimental evidence based on the pH dependence of k_{obs} confirms the predominance of small-amplitude protein fluctuations in the mechanism of exchange (9, 15, 27, 38). An important advantage of MS as an analytical tool for the measurement of hydrogen exchange is that EX1 and EX2 motions can be distinguished by examining the distribution of mass spectral peaks.

In native state hydrogen exchange experiments in the EX2 regime, the degree of protection of individual hydrogens can be quantified. As described by Bai et al. (6), the ratio of the chemical exchange rate to the observed exchange rate provides a measure of the equilibrium constant describing the distribution of open versus closed states in solution ($k_{\text{ch}}/k_{\text{obs}} \approx k_{\text{cl}}/k_{\text{op}} = 1/K_{\text{op}}$). This ratio is termed the “protection factor” (P) and is proportional to ΔG_{op} , the thermodynamic barrier over which a protein structure must cross to enable solvent exposure and subsequent hydrogen exchange (6, 7, 15). Log P typically ranges from 2 to

9 in native state proteins, suggesting motions with free energy barriers of 2–12 kcal mol⁻¹. This interpretation is an approximation that assumes that constant chemical exchange rates (k_{ch}) for hydrogens are determined solely by the primary structure and the concentration of available catalyst. However, local side chains in the three-dimensional microenvironment of the hydrogen may alter the chemical exchange rate to values that cannot be quantified easily using model compounds or peptides (47, 79, 80). Nevertheless, the approximation indicates that free energies of protein motions that lead to hydrogen exchange are consistent with low-energy fluctuations, hydrogen bond disruptions, and local unfolding events.

Hydrogen exchange studies of native state proteins are used to explore conformational properties of folded proteins. For example, hydrogen exchange rates are commonly used in NMR determinations of protein structure, where very slowly exchanging amide hydrogens are assumed to be hydrogen bonded within regions of secondary structure. Such information can be included as constraints in simulated annealing protocols for structure calculations. Another interpretation of native state exchange experiments is that the slowest exchanging amides, which typically form a core near the center of the molecule, constitute a folding core and potential nucleation site for secondary structure formation on the protein folding pathway (47, 79, 80). This has been supported by Φ analysis experiments, which characterize effects of mutations on *in vitro* folding rates (43). In general, the slowest exchanging amide hydrogens are observed on residues with the highest Φ values, which are equated with residues that nucleate first to form the folding core. This suggests that native state exchange measurements in some cases may lend insight into folding pathways.

In contrast to studies with native proteins, hydrogen exchange measurements have been used to more directly examine protein folding and unfolding mechanisms, utilizing equilibrium and pre-equilibrium approaches. We mention this broad area only briefly, as detailed reviews can be found elsewhere (15, 26, 30). Three key hydrogen exchange strategies have been used in folding studies. First, the Baldwin laboratory labeled denatured ribonuclease A with tritium and then measured exchange-out of radiolabel during folding. The results showed significant protection of backbone amides from exchange prior to complete folding of ribonuclease A, as monitored by tyrosine fluorescence measurements (67), demonstrating the presence of at least one partially structured intermediate in the folding reaction of ribonuclease A. Second, an NMR technique reported simultaneously by the Baldwin and Englander laboratories involved complete deuteration of unfolded protein at low pH, initiation of folding followed by pulse labeling with H₂O at increased pH, and quenching by decreasing pH. The results provided unequivocal support for the existence of intermediate states in the folding reactions of ribonuclease A (71) and cytochrome *c* (64). Third, a method developed by the Englander laboratory (7) subsequently identified cooperative secondary structural elements during unfolding of cytochrome *c* by measuring hydrogen exchange rates titrated over a range of low concentrations of denaturant. This important finding

established firm support for a stepwise folding pathway, in contrast to a folding energy landscape with shallow minima.

HISTORICAL PERSPECTIVE

Measurements of the incorporation of deuterium and tritium into protein molecules have been performed for more than 40 years. Lenormant & Blout were among the first to report the process of amide hydrogen exchange in their attempts to assign the 1550 cm^{-1} band in infrared spectra of protein solutions, demonstrating decreased absorbance at this wavelength upon deuterium incorporation at high pH (46). This band has been subsequently assigned to N-H bond bending. Since then, hydrogen exchange has been measured by a variety of methods. Englander (25) carried out pioneering studies using tritium and scintillation counting to measure isotope exchange into full-length proteins. Ultraviolet spectroscopy and neutron diffraction have also been used to determine exchange rates (10, 23, 54). The application and interpretation of these techniques, as well as early experiments with one-dimensional NMR, are reviewed by Barksdale & Rosenberg (9). Because deuterium is an NMR-inactive isotope, reduced areas under NMR proton absorbance peaks are used to monitor exchange of protons for deuterons at individual amides. However, the disadvantages of NMR approaches are that the experiments require large amounts of protein and that assignment of spectral peaks can be arduous. NMR techniques to analyze hydrogen exchange rates were refined by Englander (26, 29, 30), who made substantial contributions to the fields of hydrogen exchange and protein folding and reviewed these approaches.

In 1990, Chowdhury et al. (14) demonstrated the use of electrospray ionization mass spectrometry (ESI-MS) to probe the conformational distribution of cytochrome *c* in solution (14). Because MS measures mass/charge, a protein ESI-MS spectrum consists of a number of differently charged ions. The distribution of this protein charge state envelope reflects the exposure of ionizable side chains to solvent, in that greater numbers of basic side chains protonated in solution will widen the charge state distribution in the gas phase. Thus, it was shown that unfolded cytochrome *c* at low pH has a wider charge state distribution than native cytochrome *c* at higher pH. Less than a year later, Katta & Chait (42) published the first use of MS to analyze hydrogen exchange rates. Using ESI-MS, they quantified the incorporation of deuterium into bovine ubiquitin, noting that some amides remained nonexchanging even after days under denaturing conditions.

With the exception of multidimensional NMR pulse techniques, methods for measuring hydrogen exchange were limited to low resolution until Rosa & Richards (65) reported protein fragmentation by proteolysis for measuring tritium incorporation into localized regions of ribonuclease S. The approach involved complete exchange of all polar protons with tritium, followed by measurement of tritium loss through back-exchange to water at different pH values. At varying times, the reactions were quenched at pH 2.8 and the proteins digested with pepsin, generating at least six different peptides that were separated by reversed-phase high-performance liquid chromatography (HPLC). Exchange rates for different peptides were then

quantified as the loss of tritium over time. Also presented in their report was the first discussion using this medium resolution technique to identify sites of protein-peptide interactions. Later, Englander et al. (24) improved the original protocol by decreasing the temperature of the HPLC separation of peptic peptides, which minimized further back-exchange of tritium radiolabel after quenching.

Zhang & Smith (84) first reported success using protein fragment separation in HX-MS, employing fast atom-bombardment (FAB) for ionization of peptides from cytochrome *c*. The FAB-MS approach suffered from the drawback that the number of peptides recovered from a hydrogen exchange experiment was only 59%, much lower than needed for complete coverage of backbone amides. Johnson & Walsh (40) first employed ESI-MS with HPLC fragment separation in hydrogen exchange analyses. This improved amide coverage to 89% and demonstrated regions of horse skeletal muscle myoglobin, which were stabilized by heme binding *in vitro* (40). The short amount of time it took to perform this experiment, involving hours for data collection, combined with the superior coverage and micromolar quantities of protein needed for the entire experiment, made hydrogen exchange ESI-MS (HX-ESI-MS) a rapid, easy technique for analyzing protein structure and dynamics. Although the back-exchange in this experiment reached ~50%, further improvements in the MS protocol have reduced the back-exchange to 10%–20% (36, 61), in agreement with empirical measurements on model peptides (8).

Improvements in ionization methods have been accompanied by improvements in the resolution of mass spectrometers. The development of orthogonal time-of-flight mass analyzers has permitted HX-ESI-MS studies with mass resolution <5 ppm, a significant increase over the 200 ppm resolution of quadrupole and ion trap instruments (13). Sample data is presented in Figure 2. Fourier transform ion cyclotron resonance (FT-ICR) mass spectrometers provide even higher resolution of ~1 ppm (68). These instruments enable detection of lower abundance peptides in digests, providing greater coverage and peptide overlap of sequences. FT-ICR mass spectrometers also allow gas phase fragmentation of full-length proteins as they enter the orifice of the instrument, replacing fragmentation by pepsin digestion (1, 11, 31, 41). This technique, alternatively called capillary-skimmer dissociation or nozzle-skimmer dissociation, is nearly identical in theory (although more efficient in practice) to source fragmentation by non-FT-ICR ESI-MS, where low-energy collisions with gas molecules excite protein molecules to break down into smaller fragments. Protein fragmentation in the absence of the proteolysis step has the potential advantage of eliminating back-exchange from HX-MS experiments.

A mass spectral technique recently developed in the Komives laboratory to analyze hydrogen exchange is matrix-assisted laser desorption ionization (MALDI) MS (50). HX-MALDI-MS has drawbacks of high back-exchange (30%–40%) and lower coverage than ESI-MS due to less efficient ionization and overlap of peaks in complex spectra. Nevertheless, the method removes the HPLC step, which greatly speeds the rate of data collection. The first experiments using this technique identified binding sites for protein kinase inhibitor (PKI) peptide and ATP in cAMP-dependent protein kinase (PKA), and the site for thrombomodulin

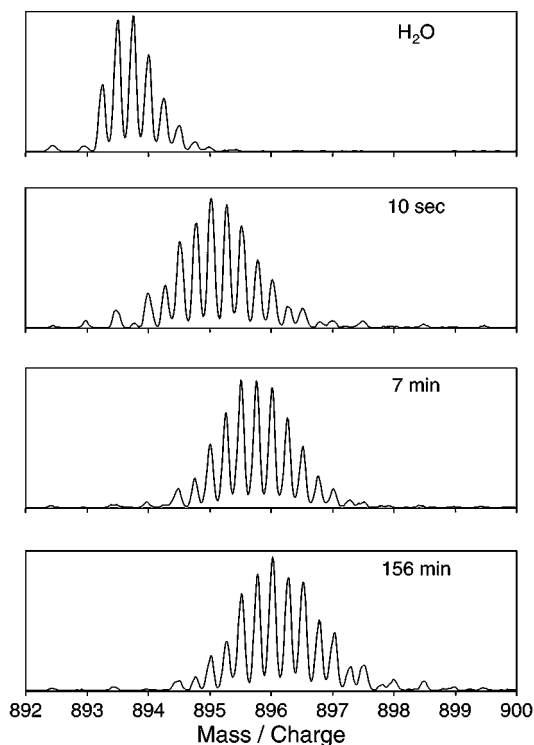


Figure 2 Example of hydrogen exchange mass spectrometric data. The mass spectrum of a MH_4^{+4} peptide ion (undeuterated monoisotopic mass = 3568.99 Da) recovered from pepsin digestion of p38 α MAPK is shown. Incubation times of protein with D_2O are indicated. Isotopic resolution is achieved using a quadrupole orthogonal time-of-flight mass spectrometer and electrospray ionization. Weighted average masses are calculated by dividing the sum of the products of the mass and intensity of each isotopic peak by the total intensity for the ion.

binding in thrombin (48, 49). In both cases, the results agreed with X-ray structural studies of co-crystallized complexes. The simplicity of data acquisition and strict agreement of the hydrogen exchange data with the available structural data make pepsin fragmentation HX-MALDI-MS an easy method for identifying putative ligand binding sites and protein-protein interfaces at medium resolution.

TECHNIQUES

In this section, we describe detailed methods for hydrogen exchange analysis by ESI-MS. Two labeling strategies are commonly used in this experiment. The general scheme for exchange-in reactions involves dissolving lyophilized protein or diluting concentrated protein solutions into D_2O and measuring increased mass

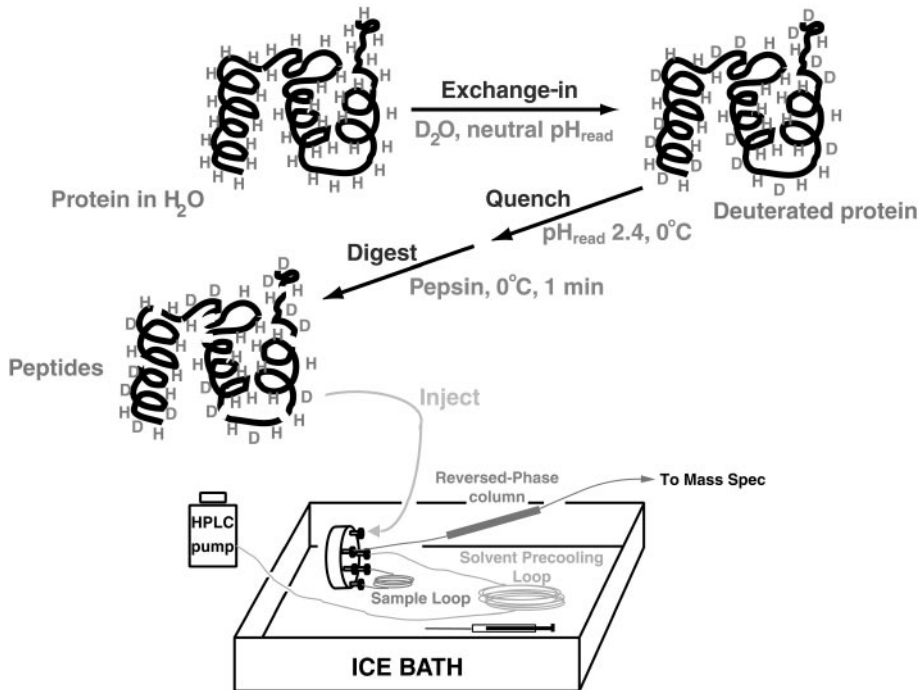


Figure 3 Apparatus for HX-MS by fragment separation. Proteins are incubated with D₂O, quenched in acid and lower temperature, and digested with pepsin. Peptides are separated with reversed-phase HPLC prior to analysis by ESI-MS. Parts of the HPLC, including the injection syringe, solvent precooling loop, sample loop, injector, and capillary column, are all immersed in ice to minimize back-exchange.

to follow deuterium incorporation (Figures 2 and 3). Alternatively, exchange-out reactions can be performed by fully deuterating the sample and pulse labeling with H₂O, measuring the exchange of protein-bound deuterium for solvent hydrogen. In binding studies performed by MALDI-MS described above, a brief exchange-in period was followed by varying times of exchange-out (48–50). This had the advantage of reducing line broadening due to deuteration of slowly exchanging amides and focusing on the rapidly exchanging amides, which typically occur on the surface of the protein and are most relevant to binding interfaces. Exchange-in and exchange-out methods are similar, and exchange-in protocols are easily adapted to measure exchange-out reactions.

Data Collection

For simplicity, we discuss our protocols used to monitor exchange-in reactions by HPLC-MS (61, 62) (Figure 3). The reactions are initiated by the addition of nine volumes of D₂O to a concentrated protein sample in buffer (pH_{read} ~ 7.4).

After varying times of exchange-in, the reaction is quenched by rapidly lowering the temperature (to 0°C) and decreasing pH_{read} to 2.4 by addition of 1:1 (v/v) citrate/succinate buffer. The protein is digested with an acid-stable protease; in most cases, pepsin is added to a final level of 1:1 (w/w) protein:pepsin.

Pepsin is a nonspecific protease that cleaves preferentially at hydrophobic residues and has some degree of secondary and tertiary structural specificity (62). Thus, a partially unfolded protein will show a different pepsin cleavage pattern than the same protein in its native state (78). Due to this unusual specificity, pepsin generates many peptides with overlapping sequence, which is of great advantage in increasing coverage of amide hydrogens in the experiment. When used with ESI-MS, we have achieved 95%–100% coverage of amide hydrogens for 42-kDa proteins. Overlapping peptides also increase the structural resolution. However, the use of pepsin in the HX-MS experiment requires peptide sequencing in order to identify the cleavage sites. Digests are analyzed by tandem mass spectrometry (MS/MS), and peptides are identified by *de novo* sequencing in combination with accurate peptide mass measurements. With current instrument and analysis software, it is possible to identify the constituent peptides of large proteins in a few hours. Pepsin can be used in solution or immobilized on a solid support. The latter was suggested by Rosa & Richards (65) in their original fragment separation paper and was demonstrated for HX-ESI-MS by the Smith laboratory (77).

In order to minimize sample handling (which impacts back-exchange as well as artifactual in-exchange), the sample is loaded into the sample loop immediately after addition of pepsin. Peptides are then injected onto a reversed-phase HPLC column in 0.05% trifluoroacetic acid (TFA) for 4 min, during which time further proteolysis occurs. Most commonly, C_{18} or C_4 reversed-phase resins are used to separate peptides, which are eluted using a gradient of acetonitrile. We use fused silica capillary columns, which can be prepared in-house at low cost (60). The entire apparatus, which includes the injector, sample loop, and column, is tightly packed in ice (Figure 3). In addition, the solvent passes through a precooling loop as it exits the pump and before entering the injector. After the binding step, the column is washed to remove salts, before diverting flow to the mass spectrometer in order to minimize problems with ionization and contamination of the orifice.

Because side chain deuterons back-exchange for hydrogen during the wash step, only deuterons at the backbone amides are retained. The maximum number of observable amides equals the number of residues in the peptide minus one, less the number of proline residues. Back-exchange of the amide hydrogen at the second amide position can also be accelerated (78). In our experience, this is not universally observed in every peptide, most likely because our protocol has been optimized to minimize back-exchange.

Following washing, peptides are eluted using a gradient of acetonitrile in 0.05% TFA. The gradient used depends on the size of the protein and complexity of the digest, and in general should be steep enough to elute the peptides quickly in order to minimize back-exchange, yet shallow enough to adequately separate the peptides. Use of a step gradient of acetonitrile loaded into the sample loop of the

injector, together with isocratic solvent delivery of 0.05% TFA/H₂O, reduces the dead time between the end of the wash step and the beginning of the gradient and also permits the incorporation of the solvent precooling loop (Figure 3). Generally, elution of the last peptide can be achieved within 20 min after quenching.

Rigorous attempts to automate the LC-MS analysis of hydrogen exchange reactions have also proven successful. Using an autosampler equipped with a dry ice cooling system, Woods & Hamuro (78) have automated the analysis of quenched, frozen reactions by HPLC-ESI-MS using a quadrupole ion trap mass spectrometer, which allows data collection at a rate of 20–50 hydrogen exchange reactions per day. Ghaemmaghami et al. (32) have also proposed methods for autosampler MALDI target plate spotting for analyzing protein stability by hydrogen exchange at rates of hundreds per day in order to find potential protein specimens for structural genomics.

The number of time points required in the HX-MS experiment depends on the application. For example, in the binding and stability studies described below, which involve large changes in solvent protection, three to five short time points (<30 min) are sufficient to draw qualitative conclusions. However, in order to quantify exchange rates for estimation of protection factors, measurements are optimal with 20–30 data points across a wide range of time. Manual sample manipulation limits the shortest time for hydrogen exchange to a few seconds. Alternative mixing approaches using rapid quench apparatuses have been reported, which extend the exchange time to the millisecond regime (20). Thus, it is currently possible to achieve millisecond to hour resolution in observed hydrogen exchange rate measurements.

Data Reduction

Two important sources of error during the LC-MS analysis of hydrogen exchange experiments must be corrected during data reduction. First, after quenching and during digestion, deuterium in the reaction mixture continues to exchange with peptide hydrogens, leading to artifactual in-exchange. Although this occurs at a slow rate due to the low pH and temperature of the mixture, it may lead to 3%–10% elevated amide deuterium incorporation. A simple control experiment is to quench the reaction at pH_{read} 2.4 prior to the addition of D₂O, followed by pepsin digestion and LC-MS analysis. The amount of artifactual in-exchange can then be corrected for by the following equations (62):

$$M_{t,\text{corr(IE)}} = (M_{t,\text{wa}} - LM_{\infty,90}) / (1 - L) \quad 1.$$

and

$$L = (M_o - M_{\text{calc}}) / (M_{\infty,90} - M_{\text{calc}}), \quad 2.$$

where $M_{t,\text{corr(IE)}}$ is the artifactual in-exchange-corrected peptide mass at time t , $M_{t,\text{wa}}$ is the observed weighted average mass at time t , M_o is the observed mass for the peptide in the control experiment, M_{calc} is the theoretical average mass of the

peptide, and $M_{\infty,90}$ is the theoretical mass of the peptide at 90% total exchange [for a complete discussion of the derivation, see (62)].

A second source of error is back-exchange, where deuterons incorporated into peptides exchange-out with hydrogen from water. Deuterons may also back-exchange with water vapor during mass spectral analysis by ESI-MS or with matrix protons by MALDI-MS. Following an estimation of the back-exchange, the data may be corrected by the following equation:

$$M_{t,\text{corr}(\text{BE})} = M_{t,\text{corr}(\text{IE})} + [\text{BE} \cdot (M_{t,\text{corr}(\text{IE})} - M_{\text{calc}})], \quad 3. \text{*Erratum}$$

where $M_{t,\text{corr}(\text{BE})}$ is the artifactual in-exchange- and back-exchange-corrected mass of the peptide at time t , BE is the fractional back-exchange, $M_{t,\text{corr}(\text{IE})}$ is the mass at time t , corrected for in-exchange, and M_{calc} is the theoretical average mass of the peptide (84).

Three methods can be used to estimate the back-exchange. First, the back-exchange following quenching can be directly measured by protein deuteration followed by digestion and mass analysis (61, 84). In cases where this method is not sufficient to achieve complete deuteration, an alternative method is to generate the peptic peptides in water and pool them after purification by reversed-phase HPLC. After lyophilization, the peptides are resuspended in D_2O and incubated for 90 min at 90°C , which enables full deuteration, and then analyzed by LC-MS after quenching. The fractional back-exchange can then be calculated for each peptide:

$$\text{BE} = (M_{\infty,90} - M_{\text{BE}})/(M_{\infty,90} - M_{\text{calc}}), \quad 4.$$

where $M_{\infty,90}$ is the theoretical mass of the peptide with 90% of the backbone amide hydrogens exchanged for deuterium (for experiments performed in 90% D_2O), M_{BE} is the observed mass of the peptide using the back-exchange experiment, and M_{calc} is the theoretical average mass of the peptide.

A second method estimates back-exchange by measuring reduction in peptide mass with varying gradients of peptide elution (62). In our experimental configuration, the back-exchange increases approximately 1% for each minute the peptide is retained on the column, leading to the following empirical equation:

$$\text{BE} = L + [(\text{peptide elution time from HPLC in min} + 6 \text{ min}) \cdot 0.01 \text{ min}^{-1}], \quad 5. \text{*Erratum}$$

where L is the fraction of artificial in-exchange from Equation 2. The third method estimates back-exchange using the measurements of chemical exchange rates from peptides free in solution:

$$\text{BE}_{\text{amide}} = 1 - [k_{\text{calc}} \cdot (\text{elution time in min})], \quad 6. \text{*Erratum}$$

where BE_{amide} is the fractional back-exchange estimate for each backbone amide hydrogen, and k_{calc} is the rate of exchange calculated for the amide hydrogen (8, 36). For each peptide the fractional back-exchange may be calculated by:

$$\text{BE} = \Sigma(\text{BE}_{\text{amide}})/(M_{\infty} - M_{\text{calc}}), \quad 7.$$

where Σ (BE_{amide}) is the sum of BE_{amide} for every amide hydrogen in the peptide, from Equation 6, M_{∞} is the theoretical average mass of the peptide with every backbone amide hydrogen exchanged for deuterium, and M_{calc} is the theoretical average mass of the peptide.

Following data correction for artifactual in-exchange and back-exchange, the time courses can be modeled by a sum of exponentials, in which each amide hydrogen exchanges with a deuteron at a given rate. In theory, each amide backbone hydrogen would be represented by a separate exponential term:

$$Y = N_{th} - e^{-k_1 t} - e^{-k_2 t} - e^{-k_3 t} - e^{-k_4 t} \dots - e^{-k_w t}, \quad 8.$$

where Y is the mass of the peptide, w is the total number of amide hydrogens (minus prolines and the amino terminal amide hydrogen), k_1 , k_2 , k_3 , k_4 , and k_w are the rates of exchange for the amide hydrogen (units: time-unit^{-1}), t is time, and N_{th} is the theoretical mass of the peptide when 100% of the amide hydrogens are in-exchanged (if the exchange reaction were carried out in 100% D_2O). However, in practice amide hydrogen exchange rates are averaged into fast, intermediate, and slow rates, and time courses can be fit to between one and three exponential terms, as shown in Figure 4.

STRUCTURAL RESOLUTION

Ideally, single amide resolution is needed to calculate protection factors in estimating free energies of exchange. This is limited with HX-MS owing to the medium resolution obtainable through proteolysis. In contrast, hydrogen exchange rates can be assigned to single amides by multidimensional NMR spectroscopy. However, whereas comprehensive coverage of all amides is usually not possible using NMR, high sequence coverage can usually be achieved by MS. In addition, the process of assigning NMR peaks can be lengthy, the concentrations of protein needed are typically much higher than physiological, and the upper mass limit for proteins is relatively low. For this reason, improved strategies are needed to achieve single amide resolution by MS and are a focus of current developments in this field.

Increased Resolution Achieved with Overlapping Peptides

An effective strategy uses peptides with overlapping sequences to deconvolute exchange rates. Because pepsin is a nonspecific protease, the degree of overlap can be significant, reaching 3 to 4 overlapping peptides for a given region of the protein molecule. Least squares fitting of time courses provide estimates of the number of amides with fast, intermediate, or slow rates. Amides in peptides can be modeled to these rates and compared with overlapping peptides to increase resolution. As an example, a collection of peptides used in a study of MAPK demonstrates the ability of overlapping sequences to improve the resolution of measurements to within 3 to 4 amino acids (Figure 5). The assigned rates were consistent with hydrogen bonding patterns in regional secondary structures identified by X-ray crystallography

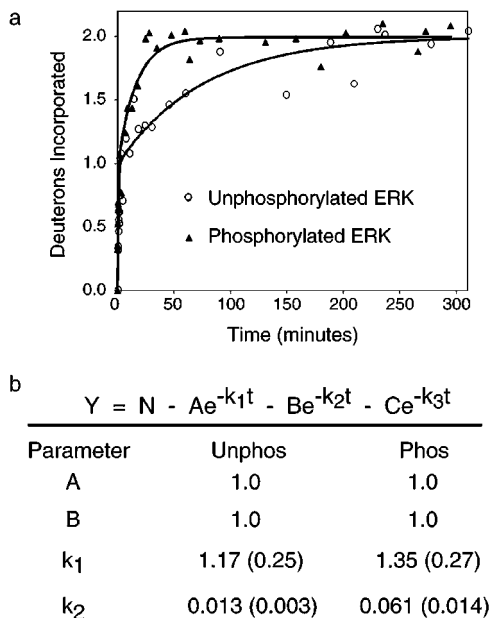


Figure 4 Data reduction. (a) Weighted average masses are calculated from isotopic peaks and plotted versus time of incubation with D_2O , as in this peptide derived from phosphorylated (\blacktriangle) and unphosphorylated (\circ) forms of ERK2. (b) Data are corrected for D_2O dilution, artifactual in-exchange, and back-exchange, then fit by nonlinear least squares to a sum of exponentials. Fitted parameters include N , the mass of the peptide at equilibrium, and A , B , and C , the number of amides exchanging, respectively, at apparent rates k_1 , k_2 , and k_3 . In this example, the data could be modeled to two amides exchanging at 1.17 and 0.013 min^{-1} , the slower of which increased to 0.061 min^{-1} following ERK2 phosphorylation.

(62, 82). Peptide sequence overlap can also be enhanced by performing pepsin digestion under slightly denaturing conditions (78), although with this approach it is important that data correction (particularly artifactual in-exchange) be performed appropriately under each experimental condition. Alternatively, overlap can be increased using multiple acid stable proteases with differing specificities (78). Combining these strategies could theoretically generate a collection of peptides that would achieve single amino acid resolution.

Tandem Mass Spectrometry

A second approach to increasing the resolution of HX-MS is to fragment peptide ions into daughter ions by collisions in the gas phase (MS/MS). By comparing weighted average masses of successive daughter ions, deuteration of individual amides should be revealed when mass increments are 1 Da greater than the residue

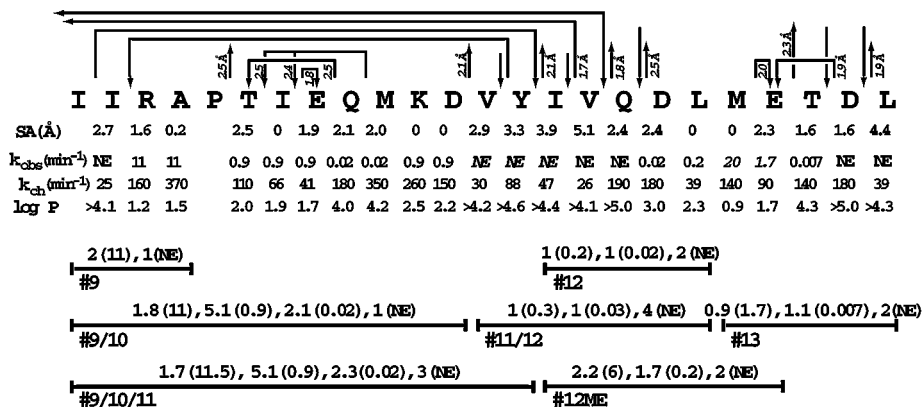


Figure 5 Increased resolution using overlapping peptic peptides. Partial digestion resulted in seven overlapping peptides in the $\beta 5$ - α D region of ERK2. At the top, arrows pointing up indicate amide hydrogen bonds and bond lengths (Å) to various acceptors at residue side chains or carbonyl oxygens are indicated. Arrows pointing down indicate hydrogen bonding to carbonyls adjacent to the amides. At the bottom, observed peptides are shown by horizontal bars, indicating stoichiometries and rates (min⁻¹) determined by nonlinear least squares. In the middle, distance to the surface of the protein and chemical exchange rate (k_{ch}) are indicated for each amide hydrogen (8). Assignment of an approximate k_{obs} to each amide is based on analysis of peptides 9, 9/10, 9/10/11, 11/12, 12, 12ME, and 13, where rates in italics indicate tentative assignments. The estimated protection factor ($P = k_{\text{obs}}/k_{\text{ch}}$) for nonexchanging (NE) amides was calculated from $k_{\text{obs}} < 0.002 \text{ min}^{-1}$.

mass. Most attempts to sequence peptides after hydrogen exchange have employed collision-induced dissociation (CID) for peptide fragmentation. The first group to report success was Anderegg et al. (3), who examined several model peptides by ESI-MS/MS and reported that it was possible to determine the extent of hydrogen exchange at individual amide hydrogens. In contrast, Johnson & Walsh (39) demonstrated shortly thereafter that model peptides in the gas phase showed complete scrambling of amide hydrogens due to migration to other positions in the peptide.

More recent reports using digested proteins (19,44) have observed localization of deuterium incorporation at specific amide hydrogens, with no extensive scrambling. In addition, an HX-ESI-MS/MS study of a model α -helical peptide incorporated into lipid qualitatively demonstrated greater deuteration at the ends of the peptide than in the lipid-protected center, although they were unable to discern whether proton migration occurred during their experiment. Studies examining full-length proteins by HX-FT-ICR-MS/MS reported that no scrambling took place during capillary-skimmer dissociation (i.e., eliminating the proteolytic step) (41).

It is important to note that in each of the aforementioned examples, nonintegral deuterium incorporation was seen at single amide positions when quantified.

Although this does not prove that scrambling took place, it could in fact be attributed to partial scrambling. Other studies examining organic model compounds have reported significant hydrogen scrambling in the gas phase, in some cases relocating from polar groups to aliphatic carbon centers (59). For the most part, these molecules are smaller than the peptides examined in the studies described above, nevertheless the conclusions may be instructive for peptides. A recent review of proton migration in aromatic compounds highlights the necessity for further experimentation and cautious interpretation (45).

In summary, the seemingly contradictory results in this area demonstrate the need for further experimentation. Rigorous experiments examining the time-dependent deuteration of individual amides with MS/MS over a range of peptide chemistries are needed to clarify the mechanisms and extent of scrambling under different experimental conditions. Furthermore, it must be remembered that at any time point an amide may only be partially exchanged and that amides will back-exchange at different rates in the same peptide because of primary and secondary structure effects. While quantitative interpretation of hydrogen exchange rates by these methods may be suspect, qualitative interpretations most likely yield valid information.

APPLICATIONS

Folding and Stability

Mass spectrometry has the particular advantage of resolving folding states, which are revealed by bimodal populations of proteins or peptides resulting from varying extents of deuteration. These reflect different populations exchanging through different mechanisms, where native forms exchange through equilibrium (EX2) mechanisms and denatured or partly unfolded forms exchange through unfolding (EX1) mechanisms. The latter can be favored by increasing denaturant concentration or by varying temperature or pH. In contrast, these populations average together and are not distinguishable when analyzed by NMR.

With its higher sensitivity and higher-upper mass limit, HX-MS has been used to great advantage in examining pathways of protein folding. For example, large portions of aldolase and cellular retinoic acid-binding protein I (CRABP-I) unfold cooperatively and exchange before refolding can take place, helping to define the structure of folding intermediates (18, 31). Transient cooperative fluctuations leading to localized unfolding have also been observed in certain genetic mutants of human lysozyme and transthyretin under conditions that favor amyloid fibril formation. Such results explain the predisposition of mutants to aggregate in patients with amyloid diseases (12, 56). Rapid quenched-flow techniques have also been incorporated to examine the earliest stabilization of secondary structure in refolding experiments (51, 70).

One of HX-MS's greatest successes is to examine folding rates in the context of the chaperones that assist folding *in vivo*. Several proteins have been studied in this

context and have revealed the mechanisms of chaperone assistance in the folding pathway for different substrates. For example, in the case of α -lactalbumin, the protein bound to the chaperone GroEL resembled the molten globule state (63), whereas human dihydrofolate reductase maintained a stable core of secondary structure during successive rounds of folding attempts by GroEL (34). This indicates that chaperones do not completely unfold proteins upon binding, but rather permit stable secondary structures in folding pathways to persist.

These methods have led to useful approaches for screening protein integrity. A clever technique developed by Ghaemmaghami and colleagues (32, 58) uses HX-MS and MALDI-MS to rapidly determine the relative stability of protein variants generated by recombinant expression. By titrating denaturant, stability can be measured from the midpoint at which hydrogen exchange becomes dominated by cooperative opening events, seen in these studies as a sharp increase in the total deuterium incorporation into full-length protein with increasing denaturant. This assay can even be performed on unpurified proteins expressed in *Escherichia coli*, as demonstrated in two studies (33, 66).

Practical applications include rapid screening for proteins suitable for structural analyses, which currently represents a significant bottleneck in genomic research initiatives. By using high-throughput techniques, these analyses could facilitate identification of expression systems among those made en masse that yield stable, folded proteins most amenable to NMR and X-ray crystallography. In addition, an ESI-MS approach has been used to characterize the ability of small molecules to inhibit transthyretin amyloid fibril formation in vitro, a promising strategy in drug development for amyloid diseases (52).

Ligand Binding, Aggregation, and Protein-Protein Interactions

A straightforward use of hydrogen exchange is to probe sites for molecular interaction by analyzing regions of solvent protection upon binding. In many cases, interfaces can be revealed by marked reductions in exchange rate caused by steric exclusion of solvent. Hydrogen exchange mass spectrometry has revealed interfaces for homomultimerization in aldolase and extracellular signal-regulated protein kinase-2 (ERK2) (36, 83). Binding interfaces for heteromeric protein-protein interactions have also been identified, illustrated by the examples of thrombomodulin-thrombin (49) and IGF1 binding protein-IGF1 (21). The technique has also proven useful for epitope mapping of monoclonal antibodies (5, 81). Although it has not been achieved to date, an important future application for HX-MS will be to map binding interfaces in large heteromultimeric protein complexes. Such an approach would provide rapid information to characterize the “interactome” and to facilitate the design of mutants and small molecules that modulate function.

Hydrogen exchange mass spectrometry with fragment separation has been used to probe ligand interactions with proteins. Heme binding to myoglobin was among the first published experiments using this method to examine the effects of small

ligand binding to a protein molecule (40). Other examples include phosphotyrosine peptide binding to SH2 domains (22), calcium binding to recoverin, calmodulin, and troponin C (55, 57, 74), and enzyme-active site interactions with small molecule inhibitors (35, 72, 73, 75). In principle, high-throughput techniques that have been described for HX-MS can be used to rapidly map protein binding sites for small molecule inhibitors (78).

Dynamics

In addition to mapping protein interfaces that become sterically protected following ligand binding, changes in protein dynamics accompanying ligand binding have been revealed by HX-MS. In many examples where hydrogen exchange measurements of ligand binding to proteins can be compared to NMR or crystallographic structures at high resolution, additional effects of ligand binding on exchange are observed, often at long distances from the site of interaction. For example, whereas heme binding to myoglobin led to decreased exchange rates that were attributable to steric exclusion of solvent based on structural evidence, binding also led to decreased exchange rates in regions of the protein located distal to the heme interface (40). This suggested that heme binding induced and stabilized secondary structure in these distal regions, which were postulated from NMR and X-ray studies to have little or no secondary structure in the apomyoglobin. Thus, when proteins bind small molecules or proteins, allosteric effects may lead to changes in the internal motions within local regions, which can be revealed in the hydrogen exchange experiment. Such motions may alter the opening/closing equilibrium that leads to exchange and therefore modulate observed exchange rates. For this reason, conclusions about the location of interaction sites that are based on regions of solvent protection must be treated cautiously.

On the other hand, such results reveal valuable information about allosteric contributions to protein motions that are still poorly understood. In studies probing the solvent-excluded thrombomodulin binding interface in thrombin, additional changes in solvent protection were observed upon binding in a surface loop proximal to the active site and distal to the binding interface (48). Lack of structural differences in this region in X-ray studies suggests that such changes may reflect allosteric effects that lead to reduced flexibility of the surface loop upon thrombomodulin binding. Allostery is also invoked in studies of cAMP binding to the type I regulatory subunit of cAMP-dependent protein kinase (2). In addition to solvent protection within the cAMP binding pocket, increased exchange rates were observed in a helical subdomain located at long distances from the binding site and implicated in catalytic subunit interactions. The results suggest that cyclic nucleotide binding promotes dissociation of regulatory and catalytic subunits by altering conformation or dynamics in the binding interface.

These studies highlight the potential of HX-MS for probing dynamic and conformational changes relevant to enzyme catalysis. This has been addressed in hypoxanthine-guanine phosphoribosyltransferase (HGPRT), where various protein-ligand complexes have been used to model enzyme intermediates (76). Global

hydrogen exchange progressively decreased in unbound enzyme, enzyme complexed with nucleotide (binary), nucleotide and substrate (ternary equilibrium complex), or transition state inhibitor. Significant protection was observed in the catalytic loop, nucleotide phosphate binding loop, and subunit interface, which was particularly pronounced in the transition state inhibitor complex. The results suggest stronger subunit interactions and reduced mobility of catalytic site loops in this model of the catalytic intermediate. Similar approaches examining other enzyme complexes with inhibitors, substrates, and cofactors revealed further evidence for loop and domain movements during catalysis (35, 72, 73, 75).

Internal protein motions have also been monitored by HX-MS in response to enzyme activation. For example, by comparing wild-type, inactive mitogen-activated protein kinase kinase-1 (MKK1) to three constitutively active mutant forms, marked increases in hydrogen exchange rates were observed in the N-terminal ATP binding lobe of the molecule (61). Although a crystallographic structure has not been reported for this kinase, overlapping peptides localized the site of increased exchange to single amides. This suggests that this region is more flexible in the active form, assuming that structural changes would affect more than one amide. Importantly, such changes were correlated with the degree of enzyme activity, and recent evidence showed that this region is the site of binding for a specific noncompetitive inhibitor of MKK1 (17).

Hydrogen exchange mass spectrometry has also been used to document motional effects following activation by phosphorylation in ERK2 (36). Phosphorylation led to altered exchange rates observed in regions far from the site of covalent modification. Comparison with corresponding X-ray structures ascribed these effects to long-distance changes in conformational mobility or flexibility upon enzyme activation. In each case, these were regions of the molecule expected either to interact with substrate or ATP, or to undergo movements during catalysis. This study represents an important step in using HX-MS to understand the effects of phosphorylation on protein dynamics.

Effects of phosphorylation have also been studied using HX-MALDI-MS in CheB, a regulator of chemotaxis in bacteria (37). Histidine phosphorylation of CheB increases its methyltransferase activity toward the CheA receptor, and attenuates signaling along the chemotaxis pathway. Phosphorylation caused increased hydrogen exchange in regions flanking the contact interface for regulatory and catalytic domains in CheB, which forms the active site. This disproved a previous model explaining activation by detachment of the two domains and disruption of the interface. The results instead suggested that activation by phosphorylation involves increased motions within regions surrounding the active site.

Together these findings indicate that ligand binding and covalent modifications communicate motional information over long distances in enzymes. Thus, HX-MS provides insight into solution behavior of proteins in a manner complimentary to the information from high-resolution structural evidence. When structural changes can be assumed to not occur, hydrogen exchange behavior can reveal perturbations in protein motions due to allostery and covalent modification.

Although the work in these systems has been an exciting advance in documenting the intramolecular motions in macromolecules, the theoretical description of these motions remains to be determined. First, it is important to understand the timescales, amplitude, and directionality of the motions sampled by hydrogen exchange. These cannot be identified from equilibrium measurements of hydrogen exchange, and despite attempts, it has not been possible so far to correlate hydrogen exchange rates with parameters from model free analyses of relaxation rates in NMR spectroscopy. These motions likely span timescales ranging from microseconds to milliseconds, the same magnitude on which enzyme catalysis takes place. In cases where rate-limiting steps involve a transient conformational change, it is possible that hydrogen exchange can sample regions of flexibility and correlated motions needed for dynamic events during catalysis.

CONCLUSIONS

From its inception, hydrogen exchange has complimented every aspect of biophysical analysis. The method provides a measure of the dynamic nature of proteins in solution, a complement to X-ray crystallography. It has the ability to distinguish different conformers in solution that are averaged in an NMR experiment. The approach also provides important insights into modes of peptide and small ligand binding in solution at physiological concentrations of protein. The sensitivity of the technique, the ease with which data is acquired and analyzed, and the quality of the data now permit hydrogen exchange experiments to be performed on large proteins and heteromultimeric systems with great success. New methods promise higher throughput, sensitivity, and mass accuracy. All these technological milestones make HX-MS an attractive method for gaining new insight into the behavior of macromolecular systems.

**The Annual Review of Biophysics and Biomolecular Structure is online at
<http://biophys.annualreviews.org>**

LITERATURE CITED

1. Akashi S, Naito Y, Takio K. 1999. Observation of hydrogen-deuterium exchange of ubiquitin by direct analysis of electrospray capillary-skimmer dissociation with Fourier transform ion cyclotron resonance mass spectrometry. *Anal. Chem.* 71:4974–80
2. Anand GS, Hughes CA, Jones JM, Taylor SS, Komives EA. 2002. Amide H²H exchange reveals communication between the cAMP- and catalytic subunit-binding sites in protein kinase A. *J. Mol. Biol.* 323:377–86
3. Anderegg RJ, Wagner DS, Stevenson CL, Borhardt RT. 1994. The mass-spectrometry of helical unfolding in peptides. *J. Am. Soc. Mass Spectrom.* 5:425–33
4. Arrington CB, Robertson AD. 2000. Correlated motions in native proteins from MS analysis of NH exchange: evidence for a

- manifold of unfolding reactions in ovomucoid third domain. *J. Mol. Biol.* 300:221–32
5. Baerga-Ortiz A, Hughes CA, Mandell JG, Komives EA. 2002. Epitope mapping of a monoclonal antibody against human thrombin by R/D-exchange mass spectrometry reveals selection of a diverse sequence in a highly conserved protein. *Protein Sci.* 11:1300–8
 6. Bai Y, Englander JJ, Mayne L, Milne JS, Englander SW. 1995. Thermodynamic parameters from hydrogen exchange measurements. *Methods Enzymol.* 259:344–56
 7. Bai Y, Sosnick TR, Mayne L, Englander SW. 1995. Protein folding intermediates: native-state hydrogen exchange. *Science* 269:192–97
 8. Bai YW, Milne JS, Mayne L, Englander SW. 1993. Primary structure effects on peptide group hydrogen-exchange. *Proteins* 17:75–86
 9. Barksdale AD, Rosenberg A. 1982. Acquisition and interpretation of hydrogen exchange data from peptides, polymers, and proteins. *Methods Biochem. Anal.* 28:1–113
 10. Bentley GA, Delepierre M, Dobson CM, Wedin RE, Mason SA, Poulsen FM. 1983. Exchange of individual hydrogens for a protein in a crystal and in solution. *J. Mol. Biol.* 170:243–47
 11. Buijs J, Hakansson K, Hagman C, Hakansson P, Oscarsson S. 2000. A new method for the accurate determination of the isotopic state of single amide hydrogens within peptides using Fourier transform ion cyclotron resonance mass spectrometry. *Rapid Commun. Mass Spectrom.* 14:1751–56
 12. Canet D, Last AM, Tito P, Sunde M, Spencer A, et al. 2002. Local cooperativity in the unfolding of an amyloidogenic variant of human lysozyme. *Nat. Struct. Biol.* 9:308–15
 13. Chernushevich IV, Loboda AV, Thomson BA. 2001. An introduction to quadrupole-time-of-flight mass spectrometry. *J. Mass Spectrom.* 36:849–65
 14. Chowdhury SK, Katta V, Chait BT. 1990. Probing conformational changes in proteins by mass-spectrometry. *J. Am. Chem. Soc.* 112:9012–13
 15. Clarke J, Itzhaki LS. 1998. Hydrogen exchange and protein folding. *Curr. Opin. Struct. Biol.* 8:112–18
 16. Connelly GP, Bai YW, Jeng MF, Englander SW. 1993. Isotope effects in peptide group hydrogen-exchange. *Proteins* 17:87–92
 17. Delaney AM, Printen JA, Chen H, Fauman EB, Dudley DT. 2002. Identification of a novel MAPKK activation domain recognized by the inhibitor PD184352. *Mol. Cell. Biol.* 22:7593–602
 18. Deng YH, Smith DL. 1998. Identification of unfolding domains in large proteins by their unfolding rates. *Biochemistry* 37: 6256–62
 19. Deng YZ, Pan H, Smith DL. 1999. Selective isotope labeling demonstrates that hydrogen exchange at individual peptide amide linkages can be determined by collision-induced dissociation mass spectrometry. *J. Am. Chem. Soc.* 121:1966–67
 20. Dharmasiri K, Smith DL. 1996. Mass spectrometric determination of isotopic exchange rates of amide hydrogens located on the surfaces of proteins. *Anal. Chem.* 68:2340–44
 21. Ehring H. 1999. Hydrogen exchange electrospray ionization mass spectrometry studies of structural features of proteins and protein/protein interactions. *Anal. Biochem.* 267:252–59
 22. Engen JR, Gmeiner WH, Smithgall TE, Smith DL. 1999. Hydrogen exchange shows peptide binding stabilizes motions in Hck SH2. *Biochemistry* 38:8926–35
 23. Englander JJ, Calhoun DB, Englander SW. 1979. Measurement and calibration of peptide group hydrogen-deuterium exchange by ultraviolet spectrophotometry. *Anal. Biochem.* 92:517–24
 24. Englander JJ, Rogero JR, Englander SW. 1985. Protein hydrogen-exchange studied

- by the fragment separation method. *Anal. Biochem.* 147:234–44
25. Englander SW. 1963. A hydrogen exchange method using tritium and Sephadex: its application to ribonuclease. *Biochemistry* 2:798–807
 26. Englander SW. 2000. Protein folding intermediates and pathways studied by hydrogen exchange. *Annu. Rev. Biophys. Biomol. Struct.* 29:213–38
 27. Englander SW, Downer NW, Teitelba H. 1972. Hydrogen-exchange. *Annu. Rev. Biochem.* 41:903–24
 28. Englander SW, Kallenbach NR. 1984. Hydrogen-exchange and structural dynamics of proteins and nucleic-acids. *Q. Rev. Biophys.* 16:521–655
 29. Englander SW, Mayne L. 1992. protein folding studied using hydrogen-exchange labeling and 2-dimensional NMR. *Annu. Rev. Biophys. Biomol. Struct.* 21:243–65
 30. Englander SW, Sosnick TR, Englander JJ, Mayne L. 1996. Mechanisms and uses of hydrogen exchange. *Curr. Opin. Struct. Biol.* 6:18–23
 31. Eyles SJ, Speir JP, Kruppa GH, Gierasch LM, Kaltashov IA. 2000. Protein conformational stability probed by Fourier transform ion cyclotron resonance mass spectrometry. *J. Am. Chem. Soc.* 122:495–500
 32. Ghaemmaghami S, Fitzgerald MC, Oas TG. 2000. A quantitative, high-throughput screen for protein stability. *Proc. Natl. Acad. Sci. USA* 97:8296–301
 33. Ghaemmaghami S, Oas TG. 2001. Quantitative protein stability measurement in vivo. *Nat. Struct. Biol.* 8:879–82
 34. Gross M, Robinson CV, Mayhew M, Hartl FU, Radford SE. 1996. Significant hydrogen exchange protection in GroEL-bound DHFR is maintained during iterative rounds of substrate cycling. *Protein Sci.* 5:2506–13
 35. Halgand F, Dumas R, Biou V, Andrieu JP, Thomazeau K, et al. 1999. Characterization of the conformational changes of acetohydroxy acid isomerase induced by the binding of Mg²⁺ ions, NADPH, and a competitive inhibitor. *Biochemistry* 38:6025–34
 36. Hoofnagle AN, Resing KA, Goldsmith EJ, Ahn NG. 2001. Changes in protein conformational mobility upon activation of extracellular regulated protein kinase-2 as detected by hydrogen exchange. *Proc. Natl. Acad. Sci. USA* 98:956–61
 37. Hughes CA, Mandell JG, Anand GS, Stock AM, Komives EA. 2001. Phosphorylation causes subtle changes in solvent accessibility at the interdomain interface of methylesterase CheB. *J. Mol. Biol.* 307:967–76
 38. Hvidt A, Johansen G, Linderstrøm-Lang K. 1960. Deuterium and ¹⁸O exchange. In *Laboratory Manual of Analytical Techniques in Protein Chemistry*, ed. P Alexander, JR Block, pp. 101–30. New York: Pergamon
 39. Johnson RS, Krylov D, Walsh KA. 1995. Proton mobility within electrosprayed peptide ions. *J. Mass Spectrom.* 30:386–87
 40. Johnson RS, Walsh KA. 1994. Mass-spectrometric measurement of protein amide hydrogen-exchange rates of apo-myoglobin and holo-myoglobin. *Protein Sci.* 3:2411–18
 41. Kaltashov IA, Eyles SJ. 2002. Crossing the phase boundary to study protein dynamics and function: combination of amide hydrogen exchange in solution and ion fragmentation in the gas phase. *J. Mass Spectrom.* 37:557–65
 42. Katta V, Chait BT. 1991. Conformational changes in proteins probed by hydrogen-exchange electrospray-ionization mass-spectrometry. *Rapid Commun. Mass Spectrom.* 5:214–17
 43. Kim KS, Fuchs JA, Woodward CK. 1993. Hydrogen exchange identifies native-state motional domains important in protein folding. *Biochemistry* 32:9600–8
 44. Kim MY, Maier CS, Reed DJ, Deinzer ML. 2001. Site-specific amide hydrogen/deuterium exchange in *E. coli* thioredoxins measured by electrospray ionization mass

- spectrometry. *J. Am. Chem. Soc.* 123:9860–66
45. Kuck D. 2002. Half a century of scrambling in organic ions: complete, incomplete, progressive and composite atom interchange. *Int. J. Mass Spectrom.* 213:101–44
46. Lenormant H, Blout ER. 1953. Origin of the absorption band at $1,550\text{ cm}^{-1}$ in proteins. *Nature* 172:770–71
47. Li R, Woodward C. 1999. The hydrogen exchange core and protein folding. *Protein Sci.* 8:1571–90
48. Mandell JG, Baerga-Ortiz A, Akashi S, Takio K, Komives EA. 2001. Solvent accessibility of the thrombin-thrombomodulin interface. *J. Mol. Biol.* 306:575–89
49. Mandell JG, Falick AM, Komives EA. 1998. Identification of protein-protein interfaces by decreased amide proton solvent accessibility. *Proc. Natl. Acad. Sci. USA* 95:14705–10
50. Mandell JG, Falick AM, Komives EA. 1998. Measurement of amide hydrogen exchange by MALDI-TOF mass spectrometry. *Anal. Chem.* 70:3987–95
51. Matagne A, Jamin M, Chung EW, Robinson CV, Radford SE, Dobson CM. 2000. Thermal unfolding of an intermediate is associated with non-Arrhenius kinetics in the folding of hen lysozyme. *J. Mol. Biol.* 297:193–210
52. McCammon MG, Scott DJ, Keetch CA, Greene LH, Purkey HE, et al. 2002. Screening transthyretin amyloid fibril inhibitors. Characterization of novel multi-protein, multiligand complexes by mass spectrometry. *Structure* 10:851–63
53. Deleted in proof
54. Nakanishi M, Nakamura H, Hirakawa AY, Tsuboi M, Nagamura T, Saijo Y. 1978. Measurement of hydrogen-exchange at tryptophan residues of a protein by stopped-flow and ultraviolet spectroscopy. *J. Am. Chem. Soc.* 100:272–76
55. Nemirovskiy O, Giblyn DE, Gross ML. 1999. Electrospray ionization mass spectrometry and hydrogen/deuterium exchange for probing the interaction of calmodulin with calcium. *J. Am. Soc. Mass Spectrom.* 10:711–18
56. Nettleton EJ, Sunde M, Lai Z, Kelly JW, Dobson CM, Robinson CV. 1998. Protein subunit interactions and structural integrity of amyloidogenic transthyretins: evidence from electrospray mass spectrometry. *J. Mol. Biol.* 281:553–64
57. Neubert TA, Walsh KA, Hurley JB, Johnson RS. 1997. Monitoring calcium-induced conformational changes in recoverin by electrospray mass spectrometry. *Protein Sci.* 6:843–50
58. Powell KD, Fitzgerald MC. 2001. Measurements of protein stability by H/D exchange and matrix-assisted laser desorption/ionization mass spectrometry using picomoles of material. *Anal. Chem.* 73:3300–4
59. Reed DR, Kass SR. 2001. Hydrogen-deuterium exchange at non-labile sites: a new reaction facet with broad implications for structural and dynamic determinations. *J. Am. Soc. Mass Spectrom.* 12:1163–68
60. Resing KA, Ahn NG. 1997. Protein phosphorylation analysis by electrospray ionization-mass spectrometry. *Methods Enzymol.* 283:29–44
61. Resing KA, Ahn NG. 1998. Deuterium exchange mass spectrometry as a probe of protein kinase activation. Analysis of wild-type and constitutively active mutants of MAP kinase kinase-1. *Biochemistry* 37:463–75
62. Resing KA, Hoofnagle AN, Ahn NG. 1999. Modeling deuterium exchange behavior of ERK2 using pepsin mapping to probe secondary structure. *J. Am. Soc. Mass Spectrom.* 10:685–702
63. Robinson CV, Gross M, Eyles SJ, Ewbank JJ, Mayhew M, et al. 1994. Conformation of GroEL-bound alpha-lactalbumin probed by mass spectrometry. *Nature* 372:646–51
64. Roder H, Elove GA, Englander SW. 1988. Structural characterization of folding intermediates in cytochrome-*c* by H-exchange

- labeling and proton NMR. *Nature* 335: 700–4
65. Rosa JJ, Richards FM. 1979. Experimental procedure for increasing the structural resolution of chemical hydrogen-exchange measurements on proteins—application to ribonuclease S-peptide. *J. Mol. Biol.* 133: 399–416
66. Rosenbaum DM, Roy S, Hecht MH. 1999. Screening combinatorial libraries of de novo proteins by hydrogen-deuterium exchange and electrospray mass spectrometry. *J. Am. Chem. Soc.* 121:9509–13
67. Schmid FX, Baldwin RL. 1979. Detection of an early intermediate in the folding of ribonuclease A by protection of amide protons against exchange. *J. Mol. Biol.* 135:199–215
68. Shen Y, Tolic N, Zhao R, Pasa-Tolic L, Li L, et al. 2001. High-throughput proteomics using high-efficiency multiple-capillary liquid chromatography with on-line high-performance ESI FTICR mass spectrometry. *Anal. Chem.* 73:3011–21
69. Swint-Kruse L, Robertson AD. 1996. Temperature and pH dependences of hydrogen exchange and global stability for ovomucoid third domain. *Biochemistry* 35:171–80
70. Tsui V, Garcia C, Cavagnero S, Siuzdak G, Dyson HJ, Wright PE. 1999. Quench-flow experiments combined with mass spectrometry show apomyoglobin folds through and obligatory intermediate. *Protein Sci.* 8:45–49
71. Udgaonkar JB, Baldwin RL. 1988. NMR evidence for an early framework intermediate on the folding pathway of ribonuclease A. *Nature* 335:694–99
72. Wang F, Blanchard JS, Tang XJ. 1997. Hydrogen exchange/electrospray ionization mass spectrometry studies of substrate and inhibitor binding and conformational changes of *Escherichia coli* dihydrodipicolinate reductase. *Biochemistry* 36:3755–59
73. Wang F, Li W, Emmett MR, Hendrickson CL, Marshall AG, et al. 1998. Conformational and dynamic changes of *Yersinia* protein tyrosine phosphatase induced by ligand binding and active site mutation and revealed by H/D exchange and electrospray ionization Fourier transform ion cyclotron resonance mass spectrometry. *Biochemistry* 37:15289–99
74. Wang F, Li W, Emmett MR, Marshall AG, Corson D, Sykes BD. 1999. Fourier transform ion cyclotron resonance mass spectrometric detection of small Ca(2+)-induced conformational changes in the regulatory domain of human cardiac troponin C. *J. Am. Soc. Mass Spectrom.* 10:703–10
75. Wang F, Scapin G, Blanchard JS, Angeletti RH. 1998. Substrate binding and conformational changes of *Clostridium glutamicum* diaminopimelate dehydrogenase revealed by hydrogen/deuterium exchange and electrospray mass spectrometry. *Protein Sci.* 7:293–99
76. Wang F, Shi W, Nieves E, Angeletti RH, Schramm VL, Grubmeyer C. 2001. A transition-state analogue reduces protein dynamics in hypoxanthine-guanine phosphoribosyltransferase. *Biochemistry* 40: 8043–54
77. Wang L, Pan H, Smith DL. 2002. Hydrogen exchange-mass spectrometry: optimization of digestion conditions. *Mol. Cell. Proteomics* 1:132–38
78. Woods VL, Hamuro Y. 2001. High resolution, high-throughput amide deuterium exchange-mass spectrometry (DXMS) determination of protein binding site structure and dynamics: utility in pharmaceutical design. *J. Cell. Biochem.* 37(Suppl.):89–98
79. Woodward C. 1993. Is the slow exchange core the protein folding core? *Trends Biochem. Sci.* 18:359–60
80. Woodward C, Simon I, Tuchsén E. 1982. Hydrogen exchange and the dynamic structure of proteins. *Mol. Cell. Biochem.* 48: 135–60
81. Yamada N, Suzuki E, Hirayama K. 2002. Identification of the interface of a large

- protein-protein complex using H/D exchange and Fourier transform ion cyclotron resonance mass spectrometry. *Rapid Commun. Mass Spectrom.* 16:293–99
82. Zhang F, Strand A, Robbins D, Cobb MH, Goldsmith EJ. 1994. Atomic structure of the MAP kinase ERK2 at 2.3 Å resolution. *Nature* 367:704–11
83. Zhang ZQ, Post CB, Smith DL. 1996. Amide hydrogen exchange determined by mass spectrometry: application to rabbit muscle aldolase. *Biochemistry* 35:779–91
84. Zhang ZQ, Smith DL. 1993. Determination of amide hydrogen-exchange by mass spectrometry—a new tool for protein-structure elucidation. *Protein Sci.* 2:522–31